



# A high-resolution typical pollution source emission inventory and pollution source changes during the COVID-19 lockdown in a megacity, China

Xue Hu<sup>1,2</sup> · Qizhen Liu<sup>3</sup> · Qingyan Fu<sup>3</sup> · Hao Xu<sup>2</sup> · Yin Shen<sup>3</sup> · Dengguo Liu<sup>3</sup> · Yue Wang<sup>4</sup> · Haohao Jia<sup>2</sup> · Jinping Cheng<sup>1,2</sup>

Received: 7 July 2020 / Accepted: 26 November 2020 / Published online: 16 April 2021

© The Author(s), under exclusive licence to Springer-Verlag GmbH Germany, part of Springer Nature 2020

## Abstract

To control the spread of COVID-19, China has imposed national lockdown policies to restrict the movement of its population since the Chinese New Year of January 2020. In this study, we quantitatively analyzed the changes of pollution sources in Shanghai during the COVID-19 lockdown; a high-resolution emission inventory of typical pollution sources including stationary source, mobile source, and oil and gas storage and transportation source was established based on pollution source data from January to February 2020. The results show that the total emissions of sulfur dioxide (SO<sub>2</sub>), nitrogen oxides (NO<sub>x</sub>), particulate matter (PM), and volatile organic compounds (VOCs) were 9520.2, 37,978.6, 2796.7, and 7236.9 tons, respectively, during the study period. Affected by the COVID-19 lockdown, the mobile source experienced the largest decline. The car mileage and oil sales decreased by about 80% during the COVID-19 lockdown (P3) when compared with those during the pre-Spring Festival (P1). The number of aircraft activity decreased by approximately 50%. The impact of the COVID-19 epidemic on industries such as iron and steel and petrochemicals was less significant, while the greater impact was on coatings, chemicals, rubber, and plastic. The emissions of SO<sub>2</sub>, NO<sub>x</sub>, PM<sub>2.5</sub>, and VOCs decreased by 11%, 39%, 37%, and 47%, respectively, during P3 when compared with those during P1. The results show that the measures to control the spread of the COVID-19 epidemic made a significant contribution to emission reductions. This study may provide a reference for other countries to assess the impact of the COVID-19 epidemic on emissions and help establish regulatory actions to improve air quality.

**Keywords** Emission inventory · COVID-19 · Pollution source · Megacity · High-resolution · Uncertainty analysis

## Introduction

The air pollution in China has become the focus of attention of scientists and the public due to frequent air pollution events in recent years (Wang et al. 2014). Air pollutant emission

inventories are essential for understanding air pollutant emission and developing effective pollution control strategies (Qi et al. 2017). Tremendous efforts have been made to establish atmospheric emission inventories of nation-scale (Wang et al. 2005) and city-scale (Zhang et al. 2008) in China. However, these emission inventories are often implemented on a yearly basis, such that the time resolution was low. An atmospheric emission inventory of high resolution is favorable for a comprehensive understanding of the changes of pollution sources, clarifying the spatial and temporal changes of pollutants, forecasting air quality, and guiding air pollution control strategies (Liu et al. 2018). Several studies have established high-resolution emission inventories for a single pollution source, such as for power plants (Chen et al. 2019), vehicles (Liu et al. 2018), and ships (Li et al. 2016). Such high-resolution emission inventories for single pollution sources often analyzed the daily or hourly variation of the emissions, while the emission inventories established for multiple pollution sources mostly

---

Responsible Editor: Lotfi Aleya

✉ Jinping Cheng  
jpc Cheng@sjtu.edu.cn

<sup>1</sup> China-UK Low Carbon College, Shanghai Jiao Tong University, Shanghai 200240, China

<sup>2</sup> School of Environmental Science and Engineering, Shanghai Jiao Tong University, Shanghai 200240, China

<sup>3</sup> Shanghai Environmental Monitor Center, Shanghai 200235, China

<sup>4</sup> Shanghai Environmental Protection Information Center, Shanghai 200235, China

demonstrated the monthly changes of pollution sources (Zhou et al. 2015; Qiu et al. 2014; Hua et al. 2019). There is a need for an accurate daily-resolution emission inventory to meet the demands of policy making for significant international events or heavy pollution weather warning when strict and temporary pollution control measures are required (Su et al. 2017).

In January 2020, COVID-19 broke out in China. To control the spread of the virus, China has imposed lockdown policies to keep social distance. This has resulted in widespread collateral effects, such as factory shutdowns, school suspensions, and banned parties. As people were required to reduce unnecessary contact with each other and remain isolated, the transportation industry was expected to be significantly affected by the COVID-19 epidemic, e.g., air traffic saw a dramatic decline of 60% (Josephs 2020). Thus, the accompanying emissions from air traffic were believed to be reduced. Additionally, the National Aeronautics and Space Administration (NASA) pollution monitoring satellite has also detected a considerable decrease in NO<sub>2</sub> concentration when compared with the concentrations before and during the outbreak of the COVID-19 epidemic (NASA 2020), which is largely attributed to the decrease in anthropogenic activities due to the strategies in containing the spread of COVID-19 in China.

To assess the impact of the containing measures of the COVID-19 spread on air quality quantitatively, a few studies have addressed the changes in air pollutant concentration (Mahato et al. 2020), and some others have analyzed data from statistical reports, such as power generation and cement production, combined with the emission inventory from previous years for simulation modeling (Li et al. 2020). According to published literature, there has been no establishment of a high-resolution emission inventory of pollution

sources, to analyze the changes of air pollutant emissions during the COVID-19 lockdown, which is very important for us to assess the impact of the COVID-19 lockdown on air quality.

In this study, we obtained activity data of several pollution sources with high time resolution and established a high-resolution atmospheric emission inventory during the period of 1 January 2020 to 29 February 2020 in Shanghai, China.

## Methods and materials

### Data sources

Pollution source activity data during the period of 1 January 2020 to 29 February 2020 were collected. The pollution source activity data used in this study were mainly provided by the Shanghai Municipal Bureau of Ecology and Environment. The pollution source activity data are shown in Table 1. The detailed emission factors are shown in Tables S1.

### Methods

#### Stationary source

For enterprises which have a continuous emission monitoring system (CEMS), the SO<sub>2</sub>, NO<sub>x</sub>, and PM emissions were calculated according to the “Specifications and test procedures for continuous emission monitoring system for SO<sub>2</sub>, NO<sub>x</sub> and particulate matter in flue gas emitted from stationary sources (HJ76-2017).” The emissions can be calculated according to Eq. (1).

$$D_i = C_i \times Q_i \times 10^{-6} \tag{1}$$

**Table 1** Pollution source activity data in this study

Category	Sub-category	Activity data description
Stationary source	Enterprises that have continuous emission monitoring system (CEMS)	Daily concentration and emissions of SO <sub>2</sub> , NO <sub>x</sub> , and PM
	Enterprises that do not have CEMS	The daily electricity consumption of industrial enterprises and the total annual electricity consumption and pollutant emissions of the last year
Mobile source	Motor vehicle	Vehicle ownership at all types and emission stages, annual mileage, vehicle operating conditions, and real-time vehicle flow
	Ship	Real-time automatic identification system (AIS) data
	Aircraft	Daily flights
Oil and gas storage and transportation source	Service stations	Daily oil sales
Dust source	Road, construction site, aggregate pile	Daily particulate concentration of dust from roads, construction sites, and aggregate pile

where  $D_i$  represents the total emissions of pollutants,  $\text{kg h}^{-1}$ ;  $C_i$  is the concentration of  $\text{SO}_2$ ,  $\text{NO}_x$ , and PM,  $\text{mg m}^{-3}$ ; and  $Q_i$  is the smoke volume,  $\text{m}^3 \text{h}^{-1}$ .

For enterprises where CEMS is not accessible, high-frequency data are generally necessary to study their emission character, but obtaining the production data timely is difficult. The electricity consumption of an enterprise is correlated to its production character. Therefore, the daily electricity consumption and the annual total electricity consumption and total pollutant emission of the industrial enterprise in last year were considered. The emissions can be calculated on the basis of Eq. (2):

$$E_j = A_j \times \frac{B_j}{D_j} \quad (2)$$

where  $E_j$  represents the emissions of pollutants, kg;  $j$  represents the industrial enterprise;  $A_j$  is the daily electricity consumption of the industrial enterprise in 2020, kW h;  $B_j$  is the total atmospheric emission of industrial enterprise in the last year, kg; and  $D_j$  is the annual electricity consumption of the industrial enterprise in the last year, kW h.

### Mobile sources

**Vehicle source** The types, emission stages, annual mileage, driving condition of each vehicle, and real-time vehicle flow were obtained. Basic emission factors of each type of vehicle were taken from the IVE model (Chen et al. 2007). The emissions can be calculated according to Eq. (3):

$$E_v = VT_{c,r} \times L_r \times EF_v \quad (3)$$

where  $E_v$  represents the emissions of pollutants,  $\text{kg h}^{-1}$ ;  $c$  represents the vehicle type;  $r$  is the road type;  $VT$  is traffic volume,  $\text{vehicle h}^{-1}$ ;  $L$  is road length, km; and  $EF_v$  is the emission factor,  $\text{kg (km}\cdot\text{vehicle)}^{-1}$ .

**Aircraft source** An aircraft flight is usually divided into two parts: landing and takeoff cycle (LTO) and cruise. The impact of aircraft flying above the atmospheric mixing layer on the air quality of the airport vicinity can be ignored, while the LTO cycle has a significant impact on the local air quality (Xu et al. 2020). The emissions can be calculated based on the number of LTO cycles according to Eq. (4):

$$E_a = A_a \times EF_a \quad (4)$$

where  $E_a$  represents the emission of pollutants, kg;  $A_a$  is the daily takeoff and landing cycles of the aircraft; and  $EF_a$  is the emission factor,  $\text{kg LTO}^{-1}$ .

**Ship source** The emissions were calculated based on automatic identification system (AIS) data. Calculation methods and

emission factors were selected by referring to relevant literature (Fan et al. 2016).

### Oil and gas storage and transportation sources

The VOC emissions from oil and gas storage and transportation were estimated by the following equation:

$$E_g = EF_g \times Q_g \times (1-\eta) \quad (5)$$

where  $E_g$  represents the emission of pollutants, kg;  $EF_g$  is the emission factor;  $Q_g$  is the daily sales of oils at service stations, kg; and  $\eta$  represents the removal efficiency of VOCs by pollution control technology.

### Uncertainty analysis

The accuracy of activity data and emission factor is vitally important for emission quantification (Zhao et al. 2010). The Monte Carlo analysis method was applied to quantify the potential uncertainty of the established emission inventory (Streets et al. 2003). The uncertainty of the emission factor and activity level were given by simulation equation, and 10,000 simulations were implemented. The upper and lower limits of 95% confidence interval were assigned to determine the uncertainty range.

## Results and discussions

### Primary air pollutant emissions

The emissions of  $\text{SO}_2$ ,  $\text{NO}_x$ ,  $\text{PM}_{2.5}$ , and VOCs from typical sources in Shanghai during the period of 1 January 2020 to 29 February 2020 are summarized in Table 2. Industrial enterprise represents the largest emission source of  $\text{PM}_{2.5}$  and VOCs, accounting for 44% and 73% of the total emissions, respectively, while contributing only 17% and 12% of the  $\text{SO}_2$  and  $\text{NO}_x$  emissions, respectively.  $\text{NO}_x$  was emitted largely from ships (61%), vehicles (23%), and industrial enterprises (12%). Ships and industrial enterprises were the two dominant sources for  $\text{SO}_2$ , accounting for 79% and 17%, respectively, while power plants accounted for only 4%. This may be because the coal-fired power plants in Shanghai had met the ultralow emission requirements in 2017, and the coal-fired power plants' pollutant emissions had been reduced significantly (Chen et al. 2019). It is noteworthy that emissions from ships account for 79%, 61%, and 32% of the total  $\text{SO}_2$ ,  $\text{NO}_x$ , and  $\text{PM}_{2.5}$  emissions, respectively. Ship emissions account for a relatively large proportion and should not be ignored. It is necessary to formulate effective control measures.

**Table 2** Emission in Shanghai from January to February 2020 (t)

Category	Sub-category	SO <sub>2</sub>	NO <sub>x</sub>	PM <sub>2.5</sub>	VOCs
Stationary source	Industrial enterprise	1587.8	4518.1	1242.1	5261.7
	Power plant	336.6	864.6	33.4	–
Mobile source	Vehicle	–	8760.2	596.9	1640.2
	Aircraft	27.7	606.7	20.9	105.5
	Ship	7568.1	23229.0	903.4	–
Oil and gas storage and transportation source	Service station	–	–	–	229.5
Total		9520.2	37978.6	2796.7	7236.9

**Analysis of pollution source changes during COVID-19**

Figure 1 shows the daily variation of atmospheric pollutant emissions from January to February 2020. To analyze the changes in intensity of the source activity before and after the implementation of strategies to contain the spread of COVID-19, the period of 1 January 2020 to 29 February 2020 was divided into four phases: pre-Spring Festival period (P1, 1.1–1.23), during the Spring Festival (P2, 1.24–1.31), during the COVID-19 lockdown (P3, 2.1–2.9), and during the resumption of work and production (P4, 2.10–2.29). There are no emission reduction measures during P1, so it can represent the general pollution status. The comparison between the changes in pollution sources during P3 and those during P1 can objectively analyze the impact of the disease on pollution sources. The Spring Festival is the most important festival in China. Traffic and industrial businesses are generally reduced sharply during the Spring Festival in most cities in China because a large number of non-local residents will leave the city and return to their hometowns for vacation. Figure 1 depicts all other pollutants except NO<sub>x</sub> with a decreasing trend during P2, and NO<sub>x</sub> emissions increased due

to the increase in ship emissions at P2. After the Spring Festival, a large number of public spaces were closed and enterprises were suspended due to the COVID-19 lockdown. Traffic flow, catering enterprises, and construction sites were also affected. Emissions of all the investigated pollutants showed a steady decreasing trend during P3. According to the COVID-19 prevention and control arrangement, industrial enterprises in Shanghai began to resume to work conditionally since February 9, and road traffic flow showed an increase since then. Correspondingly, emissions also showed an upward trend but did not reach the level during P1.

**Stationary source**

CEMS data were adopted to analyze the change of the emissions for enterprises with CEMS, while electricity consumption data were used for enterprises without CEMS.

Comparing with the emissions during P1, SO<sub>2</sub>, NO<sub>x</sub>, and PM emissions of power plants decreased by 10%, 38%, and 26% during P3, respectively.

For enterprises without CEMS, the electricity consumption during P2, P3, and P4 decreased by 16%, 19%, and 12%, respectively, when compared with that during P1. The containing measures during P3 had a considerable impact on the production activities of the enterprises. Electricity consumption has been restored to some extent during P4; however, the level was still lower than that during P1.

According to “Industry classification for national economic activities (GB/4754-2017),” industrial enterprises are divided into eight major industries: steel and iron, chemical, petrochemical, painting, rubber and plastic, printing, nonferrous, and other industries. Figure 2 shows the four-stage variation of electricity consumption in different industries. Comparing with the electricity consumption of different industry branches during P1, the electricity consumption of the steel and iron industry was almost the same and the petrochemical industry saw a reduction of 9% during P3, which were less affected by the COVID-19 lockdown. This has a certain correlation with the production character and production scale of the enterprise. The two industries are mainly composed dominantly of large enterprises, and the production character of the iron

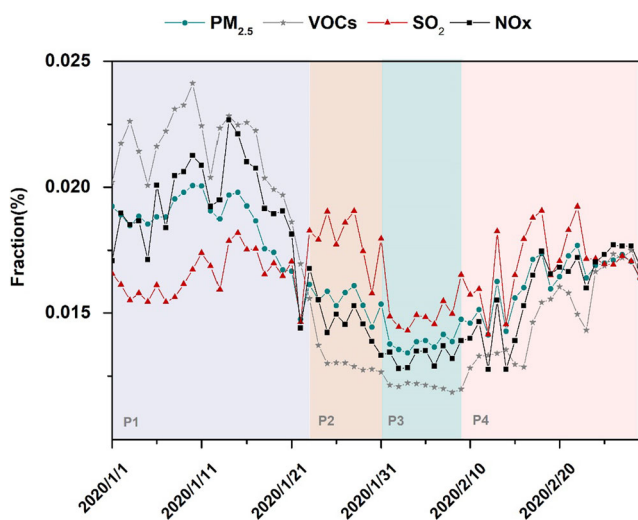


**Fig. 1** Daily temporal profiles of SO<sub>2</sub>, NO<sub>x</sub>, PM<sub>2.5</sub>, and VOC emissions from January to February 2020

and steel industry determines that the enterprises can hardly suspend their production (Huang et al. 2017). Chemical, painting, rubber and plastic, printing, nonferrous, and other industries declined by 18%, 38%, 91%, 55%, 84%, and 57%, respectively. Small-sized and medium-sized industrial enterprises experienced a significant decline in emissions during P3, which is consistent with the observation by Li et al. (2020).

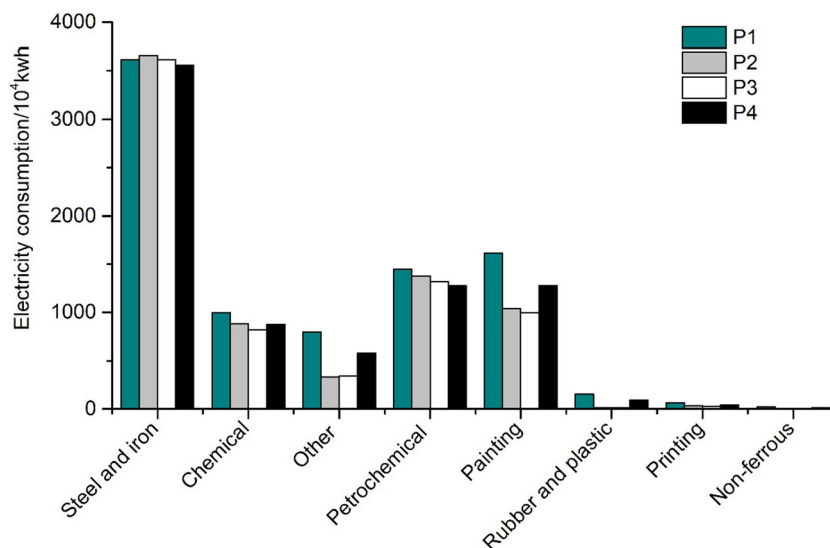
### Mobile sources

**Vehicle source** Fig. S1 shows that car mileage and oil sales were reduced sharply during COVID-19 lockdown. The mileage of diesel trucks during P1, P2, and P3 decreased by 91%, 89%, and 53%, respectively, when compared with those during P1, which was approximately consistent with the declining trend of diesel sales (85%, 80%, and 54%, respectively). The mileage of passenger cars declined by 57%, 64%, and 49%, respectively, which was basically consistent with the declining trend of gasoline sales (66%, 73%, and 64%, respectively).

The mileage of vehicles was significantly correlated with oil sales (Pearson correlation coefficient  $R = 0.97$ ,  $p < 0.01$ ). Previous studies have reported daily emissions without considering the detailed relationship between car mileage and oil sales.

**Aircraft source** The number of aircraft during P2, P3, and P4 decreased by 16%, 52%, and 71%, respectively, when compared with those during P1. Due to lockdown policies, the number of flights showed a trend of continuous decline, as is shown in Fig. S2. However, other pollution source activities showed an upward trend during P4, while aircraft movements did not, suggesting that the control measures had a great influence on the aviation industry.

**Fig. 2** Four-stage changes of electricity consumption in different industries



**Ship source** The number of ships during P2, P3, and P4 decreased by 50%, 47%, and 44%, respectively, when compared with those during P1. Fig. S3 shows that the port ships with larger emissions have a smaller decline than inland ships. The number of inland ships decreased by 84%, 82%, and 76%, respectively, while port ships dropped by 41%, 37%, and 35%, respectively.

### Dust source

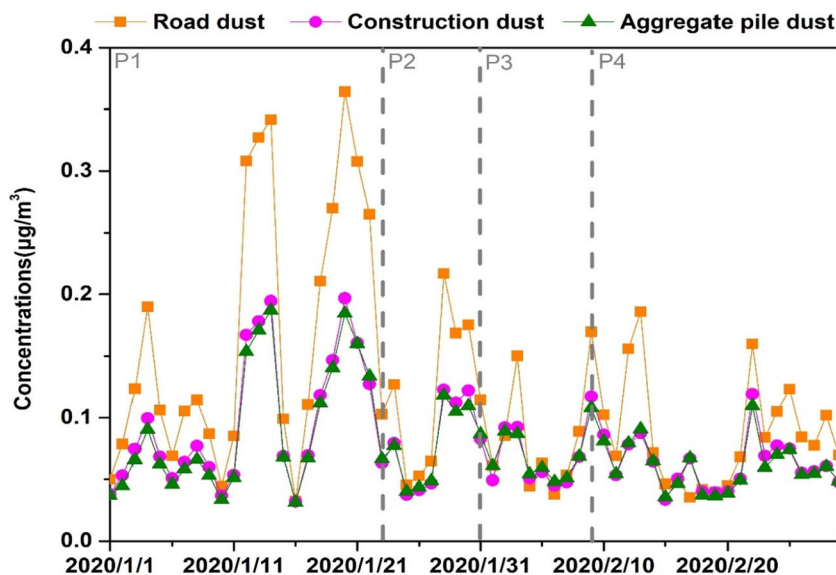
As indicated in Fig. 3, the concentration of road dust experienced the largest decline, followed by the construction dust and the aggregate pile dust during P3. The concentration of road dust during P2, P3, and P4 decreased by 27%, 47%, and 48%, respectively, when compared with those during P1. The concentration of construction dust decreased by 15%, 24%, and 32%, respectively. The concentration of aggregate pile dust decreased by 12%, 20%, and 26%, respectively.

### Emissions during different phases

The emissions of  $\text{SO}_2$ ,  $\text{NO}_x$ , VOCs, and  $\text{PM}_{2.5}$  during P2 decreased by 0.4%, 35%, 43%, and 28%, respectively, when compared with those during P1. Emissions decreased by 11%, 39%, 47%, and 37%, respectively, during P3. Emissions rebounded significantly during P4 but did not reach the P1 level, with reductions of 4%, 22%, 35%, and 37%, respectively.

The emissions of  $\text{NO}_x$  and VOCs had a sharp drop during P3 when compared with P1, and that was mainly caused by reductions in emissions from the diesel vehicles (85%) and gasoline vehicles (82%), indicating the control measures greatly reduced the pollution emissions caused by the movement of people.

**Fig. 3** Time series of concentrations of dust from 1 Jan. to 29 Feb. 2020, in Shanghai



Industrial emissions account for the majority of  $PM_{2.5}$  pollution in China (Shi et al. 2017). However, essential industries with large pollutant emissions did not curtail operations during the control period for COVID-19 (MEP 2020); the  $PM_{2.5}$  emissions from industrial and power plants decreased by 25% and 10% during P3 when compared with those in P1.

As a major pollutant emitted from the coal heating in winter (Kuerban et al. 2020), the emissions of  $SO_2$  decreased by 11%, the slowest decline during P3 when compared with P1, suggesting that coal heating activities were probably little affected by the control measures (Fig. 4).

**Uncertainty analysis**

According to Monte Carlo uncertainty analysis, the uncertainty ranges of  $SO_2$ ,  $NO_x$ ,  $PM_{2.5}$ , and VOCs are -21~28%, -34~30%, -29~27%, and -35~32%, respectively. The power plant source is relatively reliable because the majority of the activity data were obtained from the detailed facility-level census source. Uncertainties for  $SO_2$  and  $NO_x$  emissions are mainly caused by mobile sources because we are less confident of the emission estimates of those sources owing to the considerable uncertainty in emission factors and activity

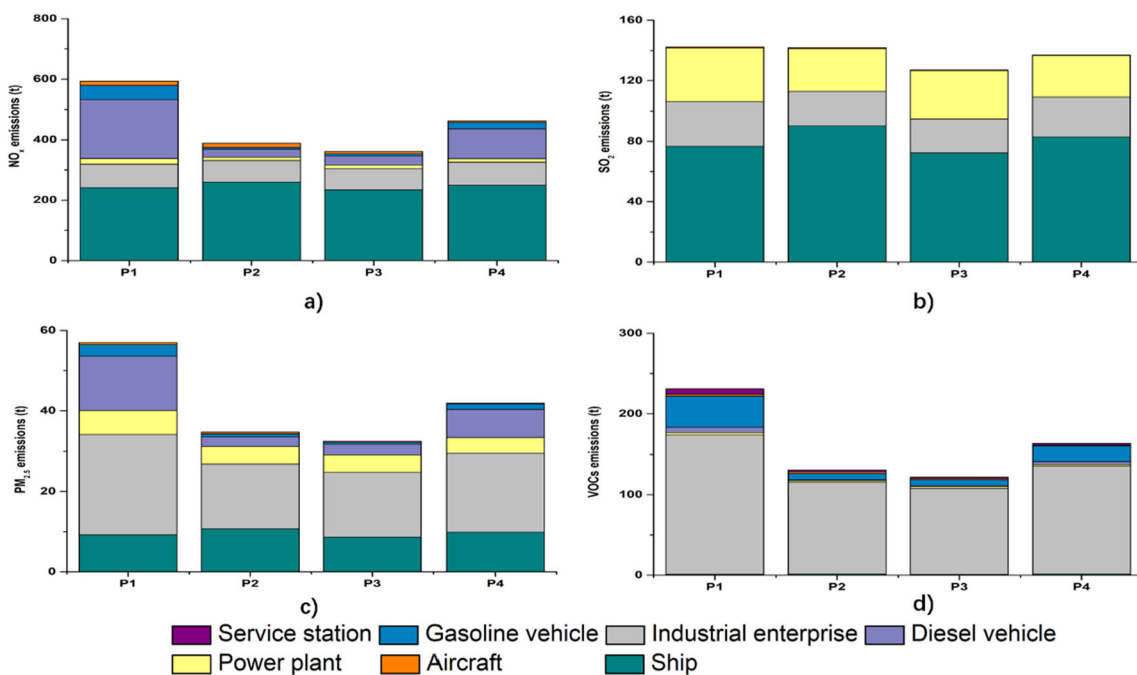


**Fig. 4** Four-stage pollutant emissions (t). (a)  $NO_x$ , (b)  $SO_2$ , (c)  $PM_{2.5}$ , (d) VOCs

levels. Industrial enterprise source is the main contributor to the uncertainties in  $PM_{2.5}$  and VOCs.

In this study, electricity consumption was applied to study the production character of the enterprise. To analyze the accuracy of this method, a large enterprise with employees > 1000 and operating income > 40 million yuan ([http://www.stats.gov.cn/tjgz/tzgb/201801/t20180103\\_1569254.html](http://www.stats.gov.cn/tjgz/tzgb/201801/t20180103_1569254.html)) was selected to analyze the correlation between the enterprise's electricity consumption and the CEMS emission data. The reason for selecting this enterprise is that the CEMS almost covers all production lines of this enterprise, which can better reflect the pollutant emissions of the enterprise.

A Pearson's correlation coefficient analysis was conducted to identify the correlation between the daily electricity consumption of the enterprise and CEMS emission data through SPSS 25.0 statistical software (IBM Corp., Armonk, NY, USA). The electricity consumption of the enterprise showed a significant positive correlation with CEMS emission data. The correlation coefficients of  $SO_2$ ,  $NO_x$ , and PM were 0.806, 0.642, and 0.843, respectively, and  $p < 0.01$ . Therefore, the electricity consumption adopted in this study can reflect the changes in production and emissions of enterprises.

### Comparison with previous studies

Emission inventories of air pollutants in Shanghai were studied only for some specific emission sources, lacking comprehensive estimation especially in the province. The average daily emissions from our study are compared to previous studies by emission sources.

For power plants, our estimated average daily emissions of  $SO_2$ ,  $NO_x$ , and PM were  $5.61 \pm 0.88$ ,  $14.41 \pm 4.25$ , and  $0.56 \pm 0.11$  t, respectively, which were lower than those of Chen et al. (2019) in 2017. The main reason for the differences was the application of an ultralow emissions policy since 2017. Additionally, the lockdown policy during P3 also has made a significant contribution to emission reductions. As for ships, the average daily emissions of  $NO_x$  were higher than those of Wan et al. (2020) in 2018, while  $SO_2$  and  $PM_{2.5}$  were lower. These differences mainly derive from emission factors and activity data.

For  $NO_x$  and VOC average daily emissions of vehicles, our estimates, applying emission factors obtained by the IVE model, were only about 60% of what Yi (2020) studied in 2018, which also applied the IVE model. This large bias could be explained by the emission reductions during the COVID-19 lockdown.

Due to the control measures during COVID-19 lockdown, the emissions from our study are generally lower than those of previous studies. The emission reductions from our study are compared with those of the other studies in the same period.

In our study, the emissions of  $SO_2$ ,  $NO_x$ , VOCs, and  $PM_{2.5}$  decreased by 11%, 39%, 47%, and 37%, respectively, during

P3 when compared with P1. Li et al. (2020) estimated the emission reductions during the epidemic control period based on changes in the activity data. The emissions of  $SO_2$ ,  $NO_x$ , VOCs, and  $PM_{2.5}$  decreased by 26%, 47%, 57%, and 46%, respectively, which were higher than those of our study, mainly due to the differences in sources and range of activity data. Wang et al. (2020) used the Community Multi-Scale Air Quality (CMAQ) model to assess emission during the outbreak of COVID-19, and the changes in transportation source and industry source were considered in their study. The emissions of pollutants decreased by about 20–40%. Our study considered more sources (power plants, aircraft, gas stations). That was the main reason why our results were higher than theirs.

### Conclusions

An emission inventory of typical air pollution sources in Shanghai was established by obtaining the pollution source data with high temporal resolution. The period of 1 January 2020 to 29 February 2020 was divided into four stages, focusing on analyzing the changes in emissions and air quality during P3. The main conclusions are as follows:

The emissions of  $SO_2$ ,  $NO_x$ , VOCs, and  $PM_{2.5}$  were 9520.2, 37,978.6, 2796.7, and 7236.9 tons, respectively, during the study period. The emissions from various pollution sources decreased significantly during P3. Mobile source depicts the largest decrease, with the car mileage and oil sales dropping by over 80%. The COVID-19 lockdown has a greater impact on the coating, chemical, rubber, and plastic industries and a relatively smaller impact on steel and iron, and petrochemical industries. The emissions of  $SO_2$ ,  $NO_x$ , VOCs, and  $PM_{2.5}$  dropped by 11%, 39%, 47%, and 37%, respectively, during P3 when compared with those in P1.

Although we recorded a temporary decline in air pollution resulting from the lockdown, it is hard to maintain this reduction after China gradually returns to work. Although travel restrictions cannot apply to air pollution control and prevention, it is possible to improve air quality by reducing non-essential individual movements by highlighting the importance of green commuting (Bao and Zhang 2020).

**Supplementary Information** The online version contains supplementary material available at <https://doi.org/10.1007/s11356-020-11858-x>.

**Acknowledgments** This study was financially supported by the National Natural Science Foundation of China (NO. 91644221 and 21777094) and the Shanghai Municipal Bureau of Ecology and Environment (NO. 2019(11)).

**Authors' contributions** Conceptualization: Xue Hu and Qizhen Liu; methodology: Xue Hu and Qingyan Fu; formal analysis and investigation: Hao Xu and Yin Shen; software: Dengguo Liu; data curation and

visualization: Yue Wang and Haohao Jia; validation: Dengguo Liu and Hao Xu; writing—original draft preparation: Xue Hu; writing—review and editing: Jinping Cheng; funding acquisition: Jinping Cheng; resources: Haohao Jia; supervision: Jinping Cheng.

**Funding** The present work was supported by the Shanghai Municipal Bureau of Ecology and Environment (NO. 2019(11)), the National Natural Science Foundation of China (NO. 91644221), and the National Natural Science Foundation of China (NO. 21777094).

**Data availability** All data generated or analyzed during this study are included in this published article and its supplementary information files.

## Compliance with ethical standards

**Ethics approval and consent to participate** Not applicable for this section.

**Consent for publication** Not applicable for this section.

**Conflict of interest** The authors declare that they have no competing interests.

## References

- Bao R, Zhang A (2020) Does lockdown reduce air pollution? Evidence from 44 cities in northern China. *Sci Total Environ* 731:139052. <https://doi.org/10.1016/j.scitotenv.2020.139052>
- Chen C, Huang C, Jing Q, Wang H, Pan H, Li L, Zhao J, Dai Y, Huang H, Schipper L (2007) On-road emission characteristics of heavy-duty diesel vehicles in Shanghai. *Atmos Environ* 41:5334–5344. <https://doi.org/10.1016/j.atmosenv.2007.02.037>
- Chen X, Liu Q, Sheng T, Li F, Xu Z, Han D, Zhang X, Huang X, Fu Q, Cheng J (2019) A high temporal-spatial emission inventory and updated emission factors for coal-fired power plants in Shanghai, China. *Sci Total Environ* 688:94–102. <https://doi.org/10.1016/j.scitotenv.2019.06.201>
- Fan Q, Zhang Y, Ma W, Ma H, Feng J, Yu Q, Yang X, Ng SKW, Fu Q, Chen L (2016) Spatial and seasonal dynamics of ship emissions over the Yangtze River Delta and East China Sea and their potential environmental influence. *Environ Sci Technol* 50:1322–1329. <https://doi.org/10.1021/acs.est.5b03965>
- Hua H, Jiang S, Sheng H, Zhang Y, Liu X, Zhang L, Yuan Z, Chen T (2019) A high spatial-temporal resolution emission inventory of multi-type air pollutants for Wuxi city. *J Clean Prod* 229:278–288. <https://doi.org/10.1016/j.jclepro.2019.05.011>
- Huang L, Hu J, Chen M, Zhang H (2017) Impacts of power generation on air quality in China—part I: an overview. *Resour Conserv Recycl* 121:103–114. <https://doi.org/10.1016/j.resconrec.2016.04.010>
- Josephs (2020) American Airlines cutting international summer schedule by 60% as coronavirus drives down demand. *CNBC News*, 2 April. <https://www.cnbc.com/2020/04/02/coronavirus-update-american-airlines-cuts-summer-international-flights-by-60percent-as-demand-suffers.html>
- Kuerban M, Waili Y, Fan F, Liu Y, Qin W, Dore AJ, Peng J, Xu W, Zhang F (2020) Spatio-temporal patterns of air pollution in China from 2015 to 2018 and implications for health risks. *Environ Pollut* 258:113659. <https://doi.org/10.1016/j.envpol.2019.113659>
- Li L, Li Q, Huang L, Wang Q, Zhu A, Xu J, Liu Z, Li H, Shi L, Li R, Azari M, Wang Y, Zhang X, Liu Z, Zhu Y, Zhang K, Xue S, Ooi MCG, Zhang D, Chan A (2020) Air quality changes during the COVID-19 lockdown over the Yangtze River Delta Region: an insight into the impact of human activity pattern changes on air pollution variation. *Sci Total Environ* 732:139282. <https://doi.org/10.1016/j.scitotenv.2020.139282>
- Li C, Yuan Z, Ou J, Fan X, Ye S, Xiao T, Shi Y, Huang Z, Ng SKW, Zhong Z, Zheng J (2016) An AIS-based high-resolution ship emission inventory and its uncertainty in Pearl River Delta region, China. *Sci Total Environ* 573:1–10. <https://doi.org/10.1016/j.scitotenv.2016.07.219>
- Liu S, Hua S, Wang K, Qiu P, Liu H, Wu B, Shao P, Liu X, Wu Y, Xue Y, Hao Y, Tian H (2018) Spatial-temporal variation characteristics of air pollution in Henan of China: localized emission inventory, WRF/Chem simulations and potential source contribution analysis. *Sci Total Environ* 624:396–406. <https://doi.org/10.1016/j.scitotenv.2017.12.102>
- Liu YH, Ma JL, Li L, Lin XF, Xu WJ, Ding H (2018) A high temporal-spatial vehicle emission inventory based on detailed hourly traffic data in a medium-sized city of China. *Environ Pollut* 236:324–333. <https://doi.org/10.1016/j.envpol.2018.01.068>
- Mahato S, Pal S, Ghosh KG (2020) Effect of lockdown amid COVID-19 pandemic on air quality of the megacity Delhi, India. *Sci Total Environ* 730:139086. <https://doi.org/10.1016/j.scitotenv.2020.139086>
- Ministry of Environmental Protection of China (2020) (MEP) Five experts focused on the causes of air pollution in the Beijing-Tianjin-Hebei region and surrounding areas during the control of Covid-19. [http://www.mee.gov.cn/gkml/sthjbgw/stbgt/201805/t20180503\\_435855.htm](http://www.mee.gov.cn/gkml/sthjbgw/stbgt/201805/t20180503_435855.htm) (in Chinese)
- NASA Goddard Space Flight Center, Airborne nitrogen dioxide plummets over China (2020) <https://earthobservatory.nasa.gov/images/146362/airborne-nitrogen-dioxide-plummets-over-china>
- Qi J, Zheng B, Li M, Yu F, Chen C, Liu F, Zhou X, Yuan J, Zhang Q, He K (2017) A high-resolution air pollutants emission inventory in 2013 for the Beijing-Tianjin-Hebei region, China. *Atmos Environ* 170:156–168. <https://doi.org/10.1016/j.atmosenv.2017.09.039>
- Qiu P, Tian H, Zhu C, Liu K, Gao J, Zhou J (2014) An elaborate high resolution emission inventory of primary air pollutants for the Central Plain Urban Agglomeration of China. *Atmos Environ* 86:93–101. <https://doi.org/10.1016/j.atmosenv.2013.11.062>
- Shi Z, Li J, Huang L, Wang P, Wu L, Ying Q, Zhang H, Lu L, Liu X, Liao H, Hu J (2017) Source apportionment of fine particulate matter in China in 2013 using a source-oriented chemical transport model. *Sci Total Environ* 601–602:1476–1487. <https://doi.org/10.1016/j.scitotenv.2017.06.019>
- Streets D, Bond T, Carmichael G et al (2003) An inventory of gaseous and primary aerosol emissions in Asia in the year 2000. *J Geophys Res* 108:8809. <https://doi.org/10.1029/2002jd003093>
- Su W, Liu C, Hu Q, Fan G, Xie Z, Huang X, Zhang T, Chen Z, Dong Y, Ji X, Liu H, Wang Z, Liu J (2017) Characterization of ozone in the lower troposphere during the 2016 G20 conference in Hangzhou. *Sci Rep* 7:17368. <https://doi.org/10.1038/s41598-017-17646-x>
- Wan Z, Ji S, Liu Y, Zhang Q, Chen J, Wang Q (2020) Shipping emission inventories in China's Bohai Bay, Yangtze River Delta, and Pearl River Delta in 2018. *Mar Pollut Bull* 151:110882. <https://doi.org/10.1016/j.marpolbul.2019.110882>
- Wang P, Chen K, Zhu S, Wang P, Zhang H (2020) Severe air pollution events not avoided by reduced anthropogenic activities during COVID-19 outbreak. *Resour Conserv Recycl* 158:104814. <https://doi.org/10.1016/j.resconrec.2020.104814>
- Wang X, Mauzerall DL, Hu Y, Russell AG, Larson ED, Woo JH, Streets DG, Guenther A (2005) A high-resolution emission inventory for eastern China in 2000 and three scenarios for 2020. *Atmos Environ* 39:5917–5933. <https://doi.org/10.1016/j.atmosenv.2005.06.051>
- Wang Y, Ying Q, Hu J, Zhang H (2014) Spatial and temporal variations of six criteria air pollutants in 31 provincial capital cities in China during 2013–2014. *Environ Int* 73:413–422. <https://doi.org/10.1016/j.envint.2014.08.016>



- Xu H, Fu Q, Yu Y, Liu Q, Pan J, Cheng J, Wang Z, Liu L (2020) Quantifying aircraft emissions of Shanghai Pudong International Airport with aircraft ground operational data. *Environ Pollut* 261: 114115. <https://doi.org/10.1016/j.envpol.2020.114115>
- Yi M (2020) Design and application of real-time vehicle emission measurement information system in Shanghai. *Environ Monit China* 36: 225–234 (in Chinese)
- Zhang Q, Xu J, Wang G, Tian W, Jiang H (2008) Vehicle emission inventories projection based on dynamic emission factors: a case study of Hangzhou, China. *Atmos Environ* 42:4989–5002. <https://doi.org/10.1016/j.atmosenv.2008.02.010>
- Zhao Y, Nielsen C, Lei Y et al (2010) Quantifying the uncertainties of a bottom-up emission inventory of anthropogenic atmospheric pollutants in China. *Atmos Chem Phys Discuss* 11:2295–2308. <https://doi.org/10.5194/acpd-10-29075-2010>
- Zhou Y, Cheng S, Lang J et al (2015) A comprehensive ammonia emission inventory with high-resolution and its evaluation in the Beijing–Tianjin–Hebei (BTH) region, China. *Atmos Environ* 106: 305–317. <https://doi.org/10.1016/j.atmosenv.2015.01.069>

**Publisher's note** Springer Nature remains neutral with regard to jurisdictional claims in published maps and institutional affiliations.